Journal of Solid State Chemistry 316 (2022) 123576

Contents lists available at ScienceDirect

Journal of Solid State Chemistry

journal homepage: www.elsevier.com/locate/jssc

Magnetic and structural properties of the $Fe_5Si_{1-x}Ge_xB_2$ system

Rebecca Clulow [a,*], Daniel Hedlund [b], Alena Vishina [c], Peter Svedlindh [b], Martin Sahlberg [a]

[a] Department of Chemistry – Ångström Laboratory, Uppsala University, Box 538, SE-751 21, Uppsala, Sweden
[b] Department of Materials Sciences and Engineering, Uppsala University, Box 35, SE-751 03, Uppsala, Sweden
[c] Department of Physics and Astronomy, Uppsala University, Box 516, SE-75120, Uppsala, Sweden

ARTICLE INFO

Keywords:
Permanent magnets
Transition metal alloys and compounds
X-ray diffraction
Magnetic measurements
Computer simulations

ABSTRACT

A series of compounds with compositions $Fe_5Si_{1-x}Ge_xB_2$ were synthesised and their structural and magnetic properties were investigated. The Mo_5SiB_2-type structure with tetragonal *I4/mcm* space group is maintained for all compounds with $x < 0.15$, which is estimated as the compositional limit of the system. The unit cell parameters expand with Ge content before reaching a plateau of $a = 5.5581(1)$ and $c = 10.3545(1)$ Å at $x = 0.15$. The saturation magnetisation (M_S) decreased slightly with increasing Ge content whilst the magnetocrystalline anisotropy energy (MAE) remains almost unaffected. The Curie temperature for all compounds studied is at 790 K whilst the spin-reorientation temperature shows suppression from 172 K to 101 K where $x = 0.15$. *Ab Initio* calculations reveal an increase in MAE for compositions up to $x = 0.25$ and a decreased magnitude of MAE of -0.14 MJ/m^3 for the hypothetical compound Fe_5GeB_2 relative to the parent compound Fe_5SiB_2.

1. Introduction

Magnetic materials are of significant interest and importance for energy conversion between mechanical and electrical energy. With growing energy demands, the need for high performance permanent magnets is ever increasing [1]. Currently, the most effective commercialised materials used include $Nd_2Fe_{14}B$, which was first reported in 1984 [2,3] and later optimized to give an unprecedented energy product of 0.474 MJ/m^3 and a saturation magnetisation of $M_S = 1.25$ MA/m [4]. However, a significant drawback lies in its use of the rare earth element Nd, and several other permanent magnets with comparable properties also utilise rare earth metals. In conjunction to this, all $Nd_2Fe_{14}B$ contains additives of Dy and Tb to increase the high temperature performance. The high and volatile price of rare earth elements accompanied by increasing demand has led to the need to develop rare earth free permanent magnets with improved properties over existing ferrite materials [5,6].

The favourable properties of the rare earth-based magnets are largely due to two factors, the spin-orbit coupling and the 3*d* elements. The spin orbit coupling between the 4*f* orbitals of the lanthanide and the 3*d* orbitals of the transition metal results in the high magnetocrystalline anisotropy energy (MAE) and resultant coercivity whilst the 3*d* elements provide the high Curie temperature (T_C) and high M_S. Potential rare earth free permanent magnets should therefore contain high concentrations of 3*d* elements to provide the high T_C and M_S required, however these compounds often have low MAE. One class of rare earth free materials which have already demonstrated these promising magnetic properties are the transition metal borides [7,8]. Among these, one potential candidate is Fe_5SiB_2 which crystallises with the Mo_5SiB_2-type structure, an ordered ternary variant of the Cr_5B_3-type structure, in the *I4/mcm* space group with unit cell parameters of $a = 5.5507(1)$ and $c = 10.3359(2)$ Å [9,10]. The compound contains the high concentration of magnetic 3*d* elements required and also crystallises in a tetragonal space group with a unique crystallographic axis which is a requirement for a high MAE. The compound possesses the high M_S required, 1.1 MA/m with a high $T_C = 760$ K but the MAE is far lower than desirable at 0.3 MJ/m^3. Another area of interest is the spin reorientation of the compound, which occurs at 172 K, where the magnetisation switches from the *c* axis to the *ab* plane [11]. This spin-reorientation has been shown to be sensitive to elemental substitution, for instance in $Fe_5Si_{1-x}P_xB_2$ when $x > 0.20$ the reorientation has been suppressed to 4–10 K [12], in Fe_4MnSiB_2/Fe_4CoSiB_2 the transition is not at all visible [10] while for $Fe_5Si_{0.75}Ge_{0.25}B_2$ it is suppressed to 60 K [13].

Several existing studies have concerned the effects of elemental substitutions upon the magnetic and structural properties of these materials with the aim of increasing the MAE whilst maximising the M_S and T_C of the system. The effect of substitution of Fe with Mn or Co has previously been investigated in several works, cobalt substitution leads to

* Corresponding author.
E-mail address: rebecca.clulow@kemi.uu.se (R. Clulow).

https://doi.org/10.1016/j.jssc.2022.123576
Received 14 June 2022; Received in revised form 2 September 2022; Accepted 5 September 2022
Available online 16 September 2022

a noticeable decrease in both the T_C and M_S, whilst the effect of Mn substitutions is similar but far less pronounced [10]. Previous studies have also investigated the effect of silicon substitution with both phosphorous and sulfur [14]. Phosphorous was found to increase the MAE but with notable decreases in both the M_S and T_C [12], A computational study also predicted an increase in MAE for sulfur containing analogues with a maximum at $Fe_5P_{0.4}S_{0.6}B_2$ [14].

An earlier study focused upon the synthesis and processing methods and their effects upon the magnetic properties of the system but also reported a compound with a nominal composition of $Fe_5Si_{0.75}Ge_{0.25}B_2$. The compound maintained the high T_C and M_S of the parent compound Fe_5SiB_2 but with an increase in the MAE to 0.5 MJ/m^3, the highest reported value in the family of Cr_5B_3-type structures [13]. However, the evolution of the magnetic properties with composition and the compositional limits of the system are yet to be explored. In this work several new compounds in the $Fe_5Si_{1-x}Ge_XB_2$ series are reported, their structures are analysed utilising a combination of powder X-ray diffraction (PXRD) and Energy dispersive X-ray spectroscopy (EDS). The evolution of their magnetic properties across the composition range is analysed and the MAE is determined using the law of approach to saturation. Furthermore, the effect of Ge substitution on the magnetic properties of the system is also investigated using *ab initio* methods and the compositional limit of the system is explored.

2. Experimental

2.1. Sample preparation

Samples were synthesised by arc melting of stoichiometric quantities of FeB (Höganas AB), Fe (Goodfellow, purity 99.0%), Si (Goodfellow, Purity 99.5%) and $FeGe_2$ powders under an argon atmosphere. $FeGe_2$ was initially prepared by arc melting of Fe (Testbourne Ltd, Purity 99.95%) and Ge (Lesker, purity 99.999%) and its structure confirmed by PXRD prior to further synthesis. The samples were re-melted four times to ensure good homogeneity before crushing into a powder and annealing as pellets in evacuated silica tubes at 1300 K for 7 days.

2.2. X-ray diffraction

The phase purity and crystal structures of the compounds were investigated by powder X-ray diffraction using a Bruker D8 diffractometer equipped with a lynx-eye position sensitive detector (PSD) using CuKα_1 radiation ($\lambda = 1.5406$ Å) at room temperature with a step size of 0.016° and a 2θ range of 20–125°. The crystal structures were analysed using Rietveld refinement [15] within the Topas 6 software program [16]. The refined parameters include the background, zero-point, scale factor, peak shape, unit cell parameters, atomic coordinates and preferred orientation (using the March-Dollase model with (110) direction), whilst ADPs remained fixed at 0.2. Powder X-ray diffraction patterns of each composition were also recorded as a function of temperature on cooling between 300 and 16 K and the evolution of unit cell parameters with temperature was investigated using Pawley refinements within the Topas 6 software program [16].

2.3. Energy dispersive X-ray spectroscopy

The composition of the samples was investigated using a Zeiss Leo 1550 field emission SEM equipped with Aztec energy dispersive X-ray detector. Data were collected on at least 10 points per sample using an accelerating voltage of 20 kV and any areas not corresponding to the main Fe_5SiB_2 phase were omitted from the estimates of phase composition.

2.4. Magnetometry

All samples were studied with a combination of a Quantum Design MPMS 5 XL system and a LakeShore 7404 vibrating sample magnetometer (VSM). Magnetisation measurements were carried out as a function of temperature and field. The temperature dependent measurements were performed in a field cooled mode with an applied field of 0.01 T, from 390 K to 10 K in the MPMS system with a cooling rate of 3 K/min. In the LakeShore system, the samples were heated to 1000 K and then cooled to 300 K with the same applied field and cooling rates. Isothermal magnetisation curves were collected at several temperatures with a maximum applied field of 5 T in the MPMS system and 1 T in the LakeShore VSM. The law of approach to saturation [17] was used to determine an effective anisotropy constant, $|K_{eff}|$ using the same method as in [11,12].

2.5. Theoretical calculations

Crystal structure relaxation was performed using the Vienna *Ab Initio* Simulation Package (VASP) [18] [–] [21] within the Projector Augmented Wave (PAW) method [22]. The Generalized Gradient Approximation (GGA) in Perdew, Burke, and Ernzerhof (PBE) form [23] was employed. The plane-wave energy cut off was set to 400 eV. A supercell approach was used to obtain the crystal structures of $Fe_5Si_{0.75}Ge_{0.25}B_2$, $Fe_5Si_{0.5}Ge_{0.5}B_2$, and $Fe_5Si_{0.25}Ge_{0.75}B_2$. Magnetic anisotropy energy (MAE) was calculated with spin-orbit coupling included as $MAE = E^{pl} - E^{c}$, where E^{c} and E^{pl} are the total energies with the magnetisation directed along and perpendicular to *c*-axis. The negative sign of MAE indicates the in-plane magnetic anisotropy.

For calculations based on experimental unit cell spin-polarised relativistic Korringa-Kohn-Rostoker (SPR-KKR) code [24] was used to obtain magnetisation and MAE by solving the Kohn-Sham equations within the Green's function formalism. MAE was calculated with the torque method [25] without considering the full-potential effects in the Atomic Sphere Approximation (ASA). 'Alloying' was treated within the coherent potential approximation (CPA) [26,27] using a single unit cell. The PBE [23] approximation was employed as exchange-correlation functional with the angular momentum cutoff of $l_{max} = 3$ in the multiple scattering expansion. The converged *k*-point grids were utilized for the self-consistent total energy calculations. Curie temperature was obtained within the mean-field approximation [28]. The exchange parameters J_{ij} were calculated using the magnetic force theorem implemented in the Liechtenstein-Katsnelson-Antropov-Gubanov formalism [29,30]. Sumo package [31] was used for the density of states (DOS) plots.

3. Results and discussion

3.1. Phase analysis

Four compositions within the $Fe_5Si_{1-x}Ge_xB_2$ system with $x = 0.05$, 0.10, 0.15 and 0.20 were synthesised. The samples were analysed by powder X-ray diffraction using the Rietveld refinement method, revealing $Fe_5Si_{1-x}Ge_xB_2$ as the predominant phase for each of the compositions a summary of the Rietveld refinement results is given in Fig. 1 and Table 1. A secondary FeB phase was observed in all samples though with less than 5 wt% for compositions where $x = 0.05$, 0.10 and 0.15. Details of the FeB phase are given in Tables S2 and S3 of the supporting information. For compositions where $x \geq 0.2$, a noticeable decrease in the phase purity is observed and the secondary FeB phase fraction increases substantially to around ~8 wt% with noticeable broadening of the peak at 45° which could indicate the presence of additional phases such as Fe_3Si as previously reported in the Fe_5SiB_2 system [11,12]. The presence of both Fe_3Si and FeB impurities suggests that the phases are not in equilibrium since these impurities don't occupy the same 3 phase region of the ternary phase diagram of Fe–Si–B. However, this effect is likely due to the significantly higher melting point of FeB relative to the other compounds, causing the FeB to crystallise first during the synthesis subsequently driving the composition to the Fe_5SiB_2/Fe_3Si region of the phase diagram. Attempts to synthesise compositions with higher Ge

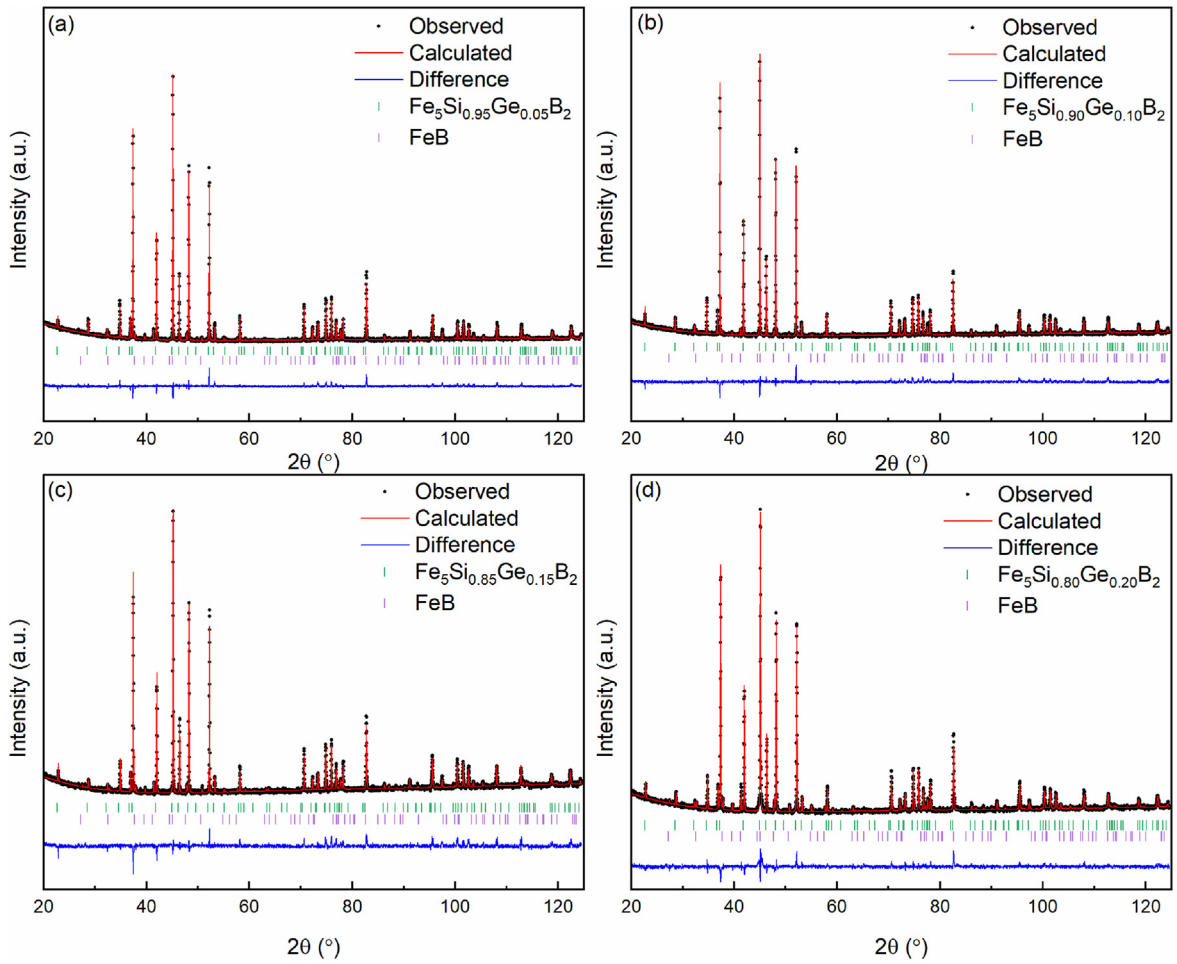

Fig. 1. Powder X-ray diffraction patterns (λ = 1.5406 Å) and Rietveld refinements of (a) $Fe_5Si_{0.95}Ge_{0.05}B_2$ $R_{wp} = 3.01$ $R_p = 2.24$ $\chi^2 = 1.41$ (b) $Fe_5Si_{0.90}Ge_{0.10}B_2$ $R_{wp} = 3.34$ $R_p = 2.56$ $\chi^2 = 1.35$ (c) $Fe_5Si_{0.85}Ge_{0.15}B_2$ $R_{wp} = 3.80$ $R_p = 2.78$ $\chi^2 = 1.57$ and (d) $Fe_5Si_{0.80}Ge_{0.20}B_2$ $R_{wp} = 3.24$ $R_p = 2.40$ $\chi^2 = 1.46$.

Table 1
Results of Rietveld refinements of $Fe_5Si_{1-x}Ge_xB_2$ (x = 0.05, 0.10, 0.15, 0.20) powder X-ray diffraction data.

x	a (Å)	c (Å)	R_{wp}	χ^2	FeB wt%
0.05	5.5518(1)	10.3388(1)	3.01	1.41	4.13(10)
0.10	5.5552(1)	10.3491(1)	3.34	1.35	2.58(10)
0.15	5.5581(1)	10.3546(1)	3.80	1.57	4.36(16)
0.20	5.5588(1)	10.3547(1)	3.24	1.46	8.04(13)

Table 2
Atomic positions and occupancies of $Fe_5Si_{0.95}Ge_{0.05}B_2$ derived from powder X-ray diffraction data collected at room temperature.

Atom	Wyckoff Position	x	y	z	Occupancy
Fe1	4c	0	0	0	1.00
Fe2	16l	0.1693(1)	0.6693(1)	0.1376(1)	1.00
Si	4a	0	0	0.25	0.95
Ge	4a	0	0	0.25	0.05
B	8h	0.6209(10)	0.1209(10)	0	1.00

content resulted in a mixture of phases suggesting a compositional limit in the amount of Ge which can be incorporated in the crystal structure using this synthesis method which is most likely limited by the significant size difference between Si and Ge.

All 4 compositions studied are isostructural to the parent compound Fe_5SiB_2 and adopt the *I4/mcm* space group. The X-ray powder diffraction data and Rietveld refinement for the first four members of the $Fe_5Si_{1-x}Ge_xB_2$ series are shown in Fig. 1 and indicate a good fit to the structural model. The refined atomic coordinates of $Fe_5Si_{0.95}Ge_{0.05}B_2$ are shown in Table 2 with full values for the other compositions provided in Table S1 in the supporting information. The evolution of the unit cell parameters with Ge content is shown in Fig. 2, both the a and c parameters initially increase with Ge content before reaching a plateau at $\sim x = 0.15$, which coincides with the maximum Ge content which could be introduced to the structure by this synthesis method. Whilst the unit cell parameters do increase with Ge content, the changes in unit cell parameters are comparatively small in comparison to the existing studies concerning P, Mn and Co substitution but are in the same order of magnitude as the previously reported compound $Fe_5Si_{0.75}Ge_{0.25}B_2$ [13].

The composition was also explored using EDS analysis, the results are summarised in Tables S4–S8 Figs. S2 and 3 in the supporting information. The compositions are in good general agreement with the nominal compositions and show increasing Ge across the series of compounds though B content is excluded from the analysis due to the poor accuracy in determining elements of low atomic weight. The analysis reveals a monotonic relationship between the nominal compositions and the estimated Ge content. The Ge content increases monotonically for $x = 0.05 - 0.15$, however Ge content does not increase for values of x greater than 0.15 suggesting something of a compositional limit for the system and synthesis method. This finding is in keeping with the PXRD analysis which contained noticeably lower levels of phase purity for compositions where $x > 0.15$.

Variable temperature X-ray diffraction was measured on each of the

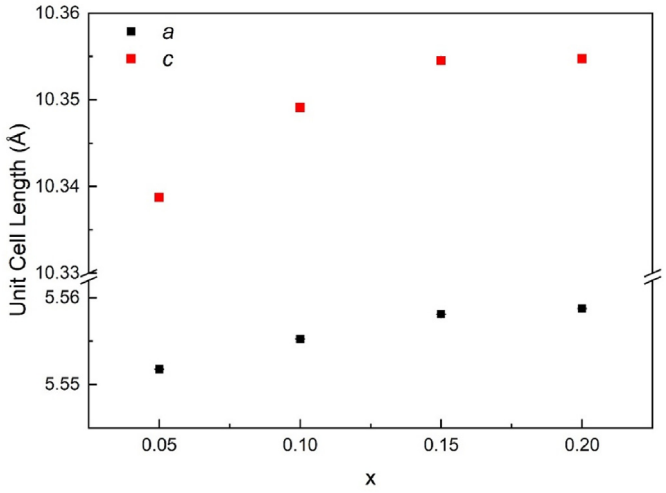

Fig. 2. Unit cell parameters of $Fe_5Si_{1-x}Ge_xB_2$ for $x = 0.05$, 0.10, 0.15 and 0.20 from Rietveld refinement of powder X-ray diffraction data collected at room temperature. Standard deviations are smaller than the symbols.

new compositions to investigate the effect of Ge content on the low temperature structure and spin reorientation temperature. Previous studies of the parent compounds Fe_5SiB_2 have found that the spin reorientation is not coupled to a change in crystal structure or symmetry. The XRD data were measured at 6 temperatures down to a minimum of 16 K, their diffraction patterns are shown in the supporting information, the unit cell parameters were also monitored across the full temperature range and in general show an expected contraction in the unit cell parameter a at lower temperatures whilst c remains almost constant as shown in Fig. 3. The unit cell parameters of the $x = 0.15$ increase slightly at lower temperatures, however, it should be noted that this composition lies on the cusp of our observed solubility limit for Ge in the Fe_5SiB_2 system which could be a contributing factor for this somewhat unusual behaviour. The analysis did not reveal evidence of any structural phase transitions at low temperature and is in agreement with the reported data for the parent compound Fe_5SiB_2 [11,12].

3.2. Magnetism

The magnetic measurements are shown in Fig. 4 and Fig. 5 and the results are summarised in Table 3. The spin reorientation of the compounds was studied using field cooled measurements as shown in Fig. 4a.

A previous neutron diffraction study shows that for Fe_5SiB_2, the cusp seen in magnetisation versus temperature can be attributed to a magnetostructural transition rather than a phase transition [11]. Our temperature dependent XRD measurements (see Fig. 3) also do not contain any evidence for a structural transition. Therefore, it is likely to assume that for the other Ge containing samples this is a magneto-structural transition. In general, the spin reorientation temperature (T_{srt}) here is shifted to lower temperatures with increasing Ge content; however, there is no clear monotonic decrease with Ge content (see Table 3).

The highest Ge content ($x = 0.20$) shows a T_{srt} at 120 K. This can be compared with Lejuene et al. [13], where they show a suppression of T_{srt} to 60 K for $Fe_5Si_{0.75}Ge_{0.25}B_2$. It should be noted that depending on the synthesis conditions, large changes were reported in both structural properties as well as magnetic properties [13]. As an example, for the same chemical composition Lejuene et al. [13] reports saturation magnetisation of 116 Am^2/kg for as spun samples, 134.4 Am^2/kg for cast-annealed samples and 158.3 Am^2/kg for melt-spun/annealed samples. In the same system, the lattice parameters (a, c) vary as 5.559(4), 10.325(5) Å for as spun, 5.551(1), 10.347(1) Å for cast-annealed and 5.549(1), 10.337(1) Å for melt-spun annealed. These differences in lattice parameters are for instance larger than what we observe in the whole temperature range of 16 K and 300 K for $x = 0.20$. It should be noted that alloying Fe_5SiB_2 with Ge may produce unexpected changes, as evident in SiGe thermoelectric materials, where neither Si or Ge possess good thermoelectric properties, whereas an alloy of these, SiGe has excellent thermoelectric properties and has been used to power some of the Voyager space missions [32].

Another property that was lifted in Lejuene et al. [13] is that T_C is not significantly affected at all by the Ge substitution. They report that their $Fe_5Si_{0.75}Ge_{0.25}B_2$ possesses T_C in the range of 791–794 K for the three different samples. In this study, samples within the range $0 \leq x \leq 0.20$ were synthesised and the effect of composition upon T_C was investigated for all compositions using magnetometry. Unexpectedly, the compounds studied in this paper also show more or less constant T_C, despite the lattice parameters varying with Ge content. Field cooled measurements can be seen in Fig. 4b, all curves are normalised to the magnetisation at 600 K, M_{600K}. All curves show a distinct minimum of dM/dT occurring around 790 K, which is the T_C reported in this study. The additional inflection at ~840 K coincides with the reported T_C of Fe_3Si suggesting trace amounts of the impurity in the samples, though at levels too low to be detected in PXRD or EDS data. The T_C of the compounds studied in this paper appear to be unaffected by the Ge content. This is in contrast to the earlier studies concerning P [12], Co [33,34], and Mn [10] substitutions. This can be attributed to the number of valence electrons in Si vs Ge, as they have similar valence shells, in contrast to the substitutions of aliovalent elements.

Fig. 5a, c shows magnetisation curves versus field at 10 K and 300 K. All samples have near zero coercivity and magnetic remanence,

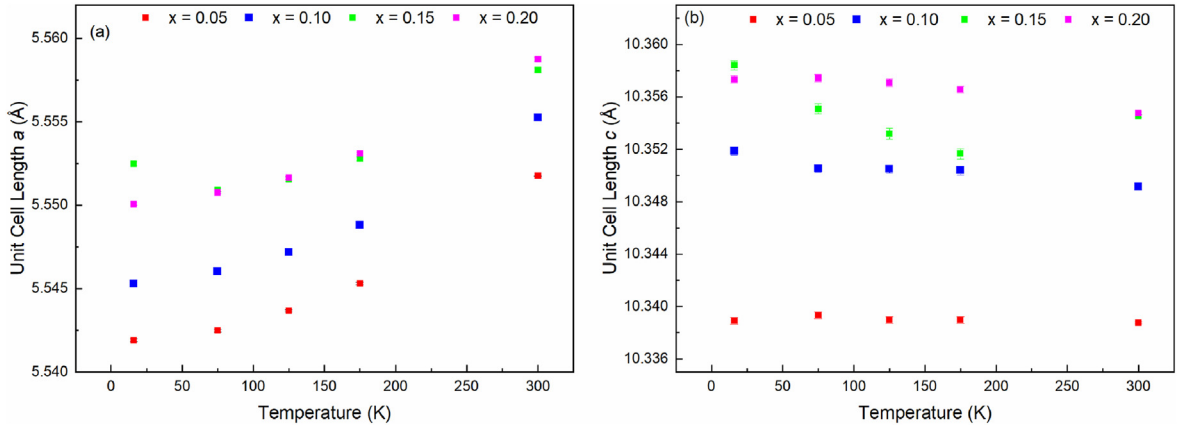

Fig. 3. Evolution of unit cell parameters of $Fe_5Si_{1-x}Ge_xB2$ ($x = 0.05$, 0.10, 0.15 and 0.2) with temperature, derived from Pawley refinement of powder X-ray diffraction data collected at 300, 175, 125, 75 and 16 K. (a) unit cell length a and (b) unit cell length c.

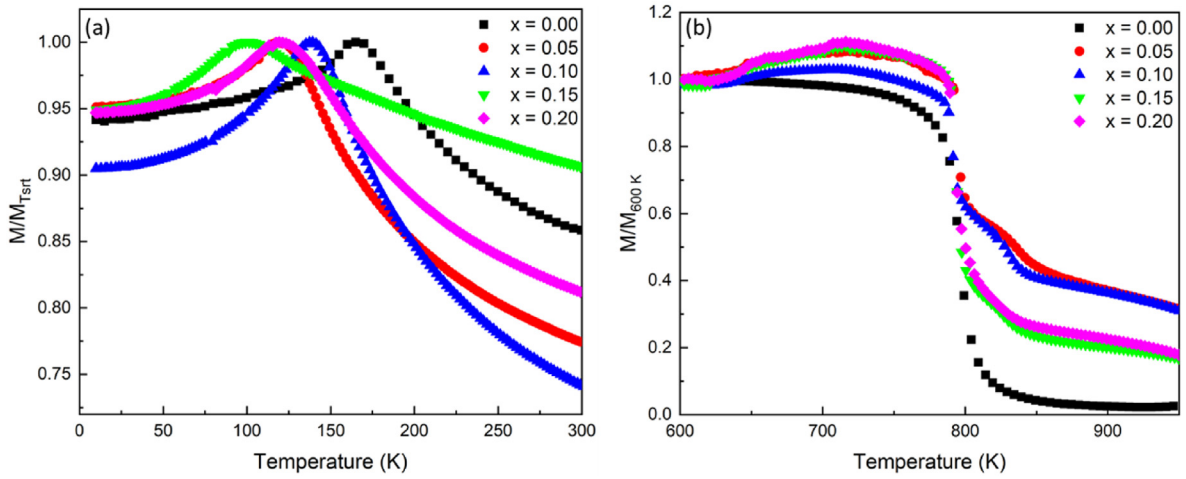

Fig. 4. (a) Magnetisation divided by the magnetisation at the spin reorientation temperature as a function of temperature in an applied field of 0.01 T in the temperature range 10–300 K. (b) Magnetisation as a function of temperature normalised by magnetisation at 600 K (M_{600K}). The data for $x = 0.0$ are taken from [12].

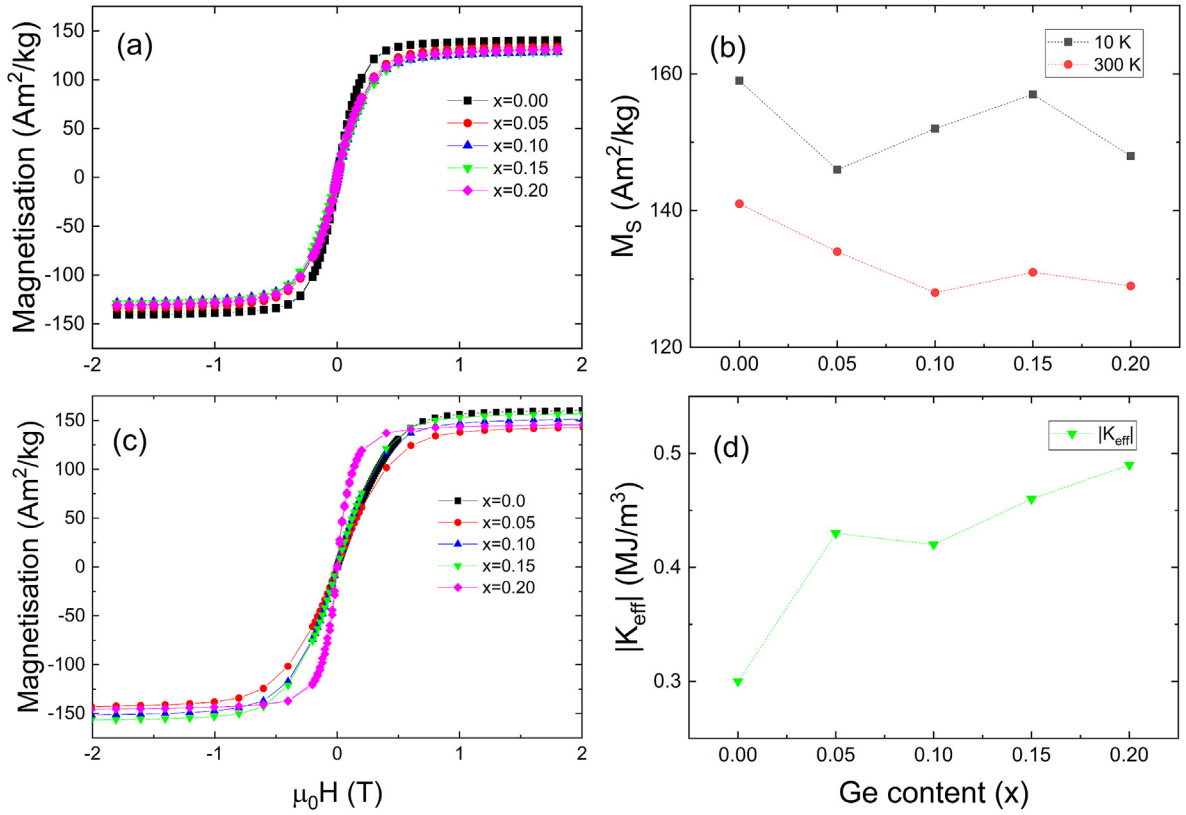

Fig. 5. Magnetisation as a function of an applied field at (a) 300 K and (c) 10 K. Saturation magnetisation versus Ge content (b) and (d) $|K_{eff}|$ as a function of Ge content. The data for $x = 0.0$ is taken from [12].

indicating that the material is magnetically soft. Fig. 5 (b) shows the saturation magnetisation versus Ge content at 10 K and 300 K, revealing a decrease of the saturation magnetisation with increasing Ge content. The general trend is that M_S only varies to a small degree at room temperature, 141 Am^2/kg for $x = 0.0$ and 129 Am^2/kg for $x = 0.20$. This is further complicated by the impurity FeB which has quite a large moment of around 1.8–2.4 μ_B/f.u [35] and is present in the highest amount in $x = 0.20$. As T_C seems unaffected by the Ge content, likely a similar argument could be made for M_S at room temperature. Here the difference in M_S is ~9%, which is largely explained by difference in phase purity and experimental uncertainty.

Lejuene et al. [13] reported that K_1 increased from 0.3 MJ/m^3 to 0.50 MJ/m^3 when part of the Si was substituted by Ge using the law of approach to saturation. In this paper, the law of approach to saturation was also used to extract an effective anisotropy constant at room temperature. The extracted value can be seen in Fig. 5d and Table 3. Overall, $|K_{eff}|$ for our samples also show that $|K_{eff}|$ increases as the Ge content increases. However, based on our experience using the law of approach to saturation this approach more serves as *tentative* description of trends rather than providing absolute values for the magnetic anisotropy. In this study, samples above $x > 0.2$ could not be synthesised. However, as both Lejuene et al. [13] and our values at least tentatively seem to show that

Table 3
Saturation magnetisation (M_S) at 10 K and room temperature, together with spin reorientation temperature, T_C and $|K_{eff}|$. The values for $x = 0.0$ are taken from [12]. The tabulated values correspond to the measured the values for the samples.

x	M_s (10 K) (Am^2/kg)	M_s (RT) (Am^2/kg)	T_{srt} (K)	T_C (K)	$\|K_{eff}\|$ (MJ/m^3)
0.00	159	141	165	790	0.30
0.05	146	134	120	790	0.43
0.10	152	128	140	790	0.42
0.15	157	131	101	790	0.46
0.20	148	129	120	790	0.49

K_1 (or $|K_{eff}|$) increases with Ge content.

In order to investigate the effect of Ge-substitution on the magnetic properties of Fe_5SiB_2 we performed the calculations in two ways – the supercell and CPA methods. As the supercell calculations are computationally expensive [36], we were only able to consider the supercell of 32 atoms constructed by multiplication of the basal unit cell and replacing one, two, and three atoms of Si with Ge. It allowed us to obtain the magnetic properties of $Fe_5Si_{0.75}Ge_{0.25}B_2$, $Fe_5Si_{0.5}Ge_{0.5}B_2$, and $Fe_5Si_{0.25}Ge_{0.75}B_2$. Lattice parameters and the internal atomic positions of these compounds were optimized using VASP both in volume and a/c ratio. All the Si in the unit cell of Fe_5SiB_2 was replaced with Ge and the unit cell relaxed to obtain crystal structure of Fe_5GeB_2.

Densities of states for Fe_5SiB_2 and Fe_5GeB_2 are given in Fig. S4. We can see, that the substitution of Si with Ge has no significant effect. The dominant role around the Fermi energy is played by *3d* orbitals. The majority spin channels are nearly fully occupied while the observed spin-splitting (proportional to the magnetic moment) is similar for both compounds. Fig. 6 shows the Fe–Fe exchange interactions is Fe_5SiB_2 and Fe_5GeB_2. The dominating interactions are positive, favouring the ferromagnetic orientation of the spins, and are similar in size, which explains the fact that the T_C observed in the experiment remains almost unchanged as Ge is added to the system.

Table 4 shows the structural and magnetic properties for the relaxed $Fe_5Si_{1-x}Ge_xB_2$ ($x = 0.00, 0.25, 0.50, 0.75$) and Fe_5GeB_2. We see the gradual increase in the values of a and c with Ge concentration up to $a = 5.552$ Å, $c = 10.569$ Å for the hypothetical compound Fe_5GeB_2, which are comparable to our reported values of $a = 5.5587$ (1) and $c = 10.3547$ (1) Å for $Fe_5Si_{0.8}Ge_{0.2}B_2$ though with a slight deviation in unit cell length c. It should be noted that PBE, while remaining the best GGA functional for most solids with 3*d* transition metals, tends to overestimate the lattice constants [37]. Saturation magnetisation shows no significant change as Si is replaced with germanium and agrees well with the experimental values. The MAE remains almost constant for Fe_5SiB_2 and $Fe_5Si_{0.75}Ge_{0.25}B_2$ at around 0.33 MJ/m^3 but decreases (in the absolute value) to −0.14 MJ/m^3 for Fe_5GeB_2. As our theoretical values are lower than measured ones, we performed the CPA calculations for the crystal structures and Ge concentrations obtained experimentally. This approach allows us consider the smaller values of x within a single unit cell. Since, according to the measurements presented in Fig. 2, crystal structure parameters seem to plateau as Ge concentration increases, we performed an additional calculation for $x = 0.25$ with the unit cell parameter measured for $x = 0.20$. The result is given in Table 5. Saturation magnetisation underestimates the experimental values slightly and varies insignificantly with x, similar to the calculations performed with VASP. MAE increases from −0.54 MJ/m^3 for $x = 0.05$ to −0.62 MJ/m^3 for $x = 0.25$. To explain the difference in magnetic anisotropy between the values obtained with the supercell and CPA methods, we performed an additional SPRKKR calculation for the a and c calculated for $Fe_5Si_{0.75}Ge_{0.25}B_2$ with structure relaxation in VASP, see Table 5. The resulting value is −0.29 MJ/m^3. Similar to Fe_5SiB_2[12] and Fe_5PB_2[31], MAE of Fe_5GeB_2 seem to be extremely sensitive to the unit volume. A VASP calculation was performed to see the change in magnetic anisotropy with the unit cell volume, see Fig. S5. The result is very close to the behaviour of MAE in Fe_5SiB_2[12] and Fe_5PB_2[31]. With the decrease in volume, magnetic anisotropy decreases in value and eventually changes its sign becoming uniaxial. As expected for the mean-field values of T_C, it is overestimated. However, similar to the experiment, there is no significant change in its value.

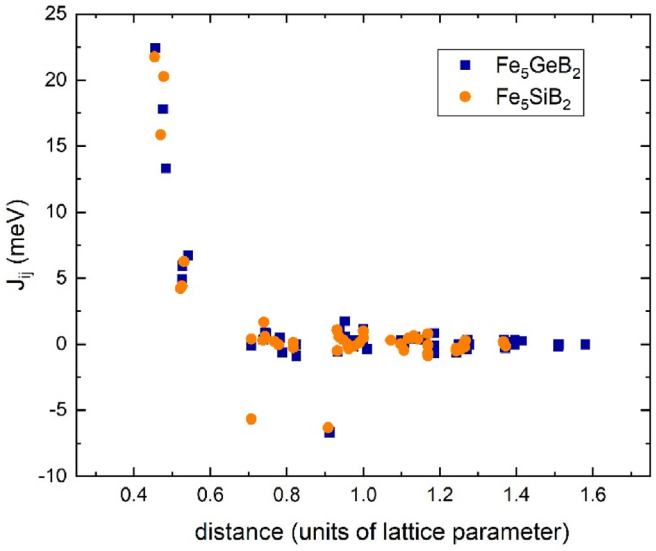

Fig. 6. Fe–Fe exchange coupling parameters for Fe_5SiB_2 and Fe_5GeB_2 plotted as a function of distance between Fe atoms.

Table 4
Lattice parameters, saturation magnetisation, and MAE calculated for the relaxed structures $Fe_5Si_{1-x}Ge_xB_2$ with VASP using the supercell method.

x	a (Å)	c (Å)	M_s (Am^2/kg)	MAE (MJ/m^3)
0.00	5.509	10.293	155.8	−0.33
0.25	5.523	10.357	149.0	−0.34
0.50	5.536	10.440	142.5	−0.25
0.75	5.545	10.497	136.7	−0.24
1.00	5.552	10.569	137.3	−0.14

Table 5
Saturation magnetisation, MAE, and T_C calculated for the experimental crystal structures $Fe_5Si_{1-x}Ge_xB_2$ with CPA and SPRKKR code. For $x = 0.25$ the unit cell parameter measured for $x = 0.20$ were used. The last line shows a calculation performed for the unit cell relaxed with VASP.

x	M_s (Am^2/kg)	MAE (MJ/m^3)	T_C (K)
0.05	137.7	−0.544	903
0.10	137.5	−0.633	911
0.15	138.9	−0.688	926
0.20	137.6	−0.623	920
0.25	136.7	−0.623	919
0.25 (rel)	134.3	−0.291	

4. Conclusions

Four new compounds within the $Fe_5Si_{1-x}Ge_xB_2$ series with $x = 0.05$, 0.10, 0.15 and 0.20 have been synthesised. The compounds are isostructural with the parent compound Fe_5SiB_2 and adopt the *I4/mcm* space group. Each of the compositions contained a few percent of FeB impurity phase but expansion of the unit cell coupled with EDS and magnetometry data show clear evidence for the incorporation of Ge into the crystal structure. Whilst Ge has been incorporated into the compounds, it appears to be limited to relatively small amounts of Ge <~15%. Magnetometry reveals a slight decrease in M_S with increasing Ge content whilst

the MAE is almost unaffected by Ge content. The T_{srt} is supressed at higher amounts of Ge but the T_C remains constant 790 K in contrast to the earlier studies regarding P, Mn and Co substitution. *Ab initio* calculations reveal an increase in MAE up to $x = 0.25$ and subsequent decrease to the value of -0.14 MJ/m^3 for the hypothetical compound Fe_5GeB_2 suggesting that further Ge substitution is unlikely to result in improved magnetic properties.

CRediT authorship contribution statement

Rebecca Clulow: Conceptualization, Investigation, Writing – original draft, Writing – review & editing, Visualization. **Daniel Hedlund:** Investigation, Writing – original draft, Writing – review & editing, Visualization. **Alena Vishina:** Investigation, Writing – original draft, Writing – review & editing, Visualization. **Peter Svedlindh:** Supervision, Writing – review & editing. **Martin Sahlberg:** Supervision, Writing – review & editing.

Declaration of competing interest

The authors declare that they have no known competing financial interests or personal relationships that could have appeared to influence the work reported in this paper.

Data availability

Data will be made available on request.

Acknowledgements

The authors acknowledge the support of the Swedish Foundation for Strategic Research (SSF, contract EM-16-0039). We acknowledge Myfab Uppsala for providing facilities and experimental support. Myfab is funded by the Swedish Research Council (2019-00207). Dr Pedro Berastegui is acknowledged for his guidance during synthesis.

Appendix A. Supplementary data

Supplementary data to this article can be found online at https://doi.org/10.1016/j.jssc.2022.123576.

References

[1] O. Gutfleisch, M.A. Willard, E. Brück, C.H. Chen, S.G. Sankar, J.P. Liu, Adv. Mater. 23 (2011) 821–842.
[2] J.J. Croat, J.F. Herbst, R.W. Lee, F.E. Pinkerton, J. Appl. Phys. 55 (1984) 2078–2082.
[3] M. Sagawa, S. Fujimara, N. Togawa, H. Yamamoto, T. Matsuura, J. Appl. Phys. 55 (1984) 2083.
[4] Y. Matsuura, J. Magn. Magn Mater. 303 (2006) 344–347.
[5] J. Cui, M. Kramer, L. Zhou, F. Liu, A. Gabay, G. Hadjipanayis, B. Balasubramanian, D. Sellmyer, Acta Mater. 158 (2018) 118–137.
[6] L.H. Lewis, F. Jiménez-Villacorta, Metall. Mater. Trans. A Phys. Metall. Mater. Sci. 44A (2013) S2–S20.
[7] P. Shankhari, O. Janka, R. Pöttgen, B.P.T. Fokwa, J. Am. Chem. Soc. 143 (2021) 4205–4212.
[8] Y. Zhang, G.J. Miller, B.P.T. Fokwa, Chem. Mater. 29 (2017) 2535–2541.
[9] B. Aronsson, G. Lundgren, S.E. Hansen, R. Sömme, E. Stenhagen, H. Palmstierna, Acta Chem. Scand. 13 (1959) 433–441.
[10] M.A. McGuire, D.S. Parker, J. Appl. Phys. 118 (2015), 163903.
[11] J. Cedervall, S. Kontos, T.C. Hansen, O. Balmes, F.J. Martinez-Casado, Z. Matej, P. Beran, P. Svedlindh, K. Gunnarsson, M. Sahlberg, J. Solid State Chem. 235 (2016) 113–118.
[12] D. Hedlund, J. Cedervall, A. Edström, M. Werwiński, S. Kontos, O. Eriksson, J. Rusz, P. Svedlindh, M. Sahlberg, K. Gunnarsson, Phys. Rev. B 96 (2017), 094433.
[13] B.T. Lejeune, R. Barua, I.J. McDonald, A.M. Gabay, L.H. Lewis, G.C. Hadjipanayis, J. Alloys Compd. 731 (2018) 995–1000.
[14] M. Werwiński, S. Kontos, K. Gunnarsson, P. Svedlindh, J. Cedervall, V. Höglin, M. Sahlberg, A. Edström, O. Eriksson, J. Rusz, Phys. Rev. B 93 (2016) 1–10.
[15] H.M. Rietveld, J. Appl. Crystallogr. 2 (1969) 65–71.
[16] A.A. Coelho, J. Appl. Crystallogr. 51 (2018) 210–218.
[17] S. Chikazumi, Physics of Ferromagnetism, vol. 1, Clarendon Press, 1997.
[18] G. Kresse, J. Hafner, Phys. Rev. B 47 (1993) 558–561.
[19] G. Kresse, J. Hafner, Phys. Rev. B 49 (1994) 14251–14269.
[20] G. Kresse, J. Furthmüller, Comput. Mater. Sci. 6 (1996) 15–50.
[21] G. Kresse, J. Furthmüller, Phys. Rev. B 54 (1996), 11169.
[22] P.E. Blöchl, Phys. Rev. B 50 (1994) 17953–17979.
[23] J.P. Perdew, K. Burke, M. Ernzerhof, Phys. Rev. Lett. 77 (1996) 3865–3868.
[24] H. Ebert, D. Ködderitzsch, J. Minár, Rep. Prog. Phys. 74 (2011), 096501.
[25] X. Wang, R. Wu, D. Wang, A.J. Freeman, Phys. Rev. B Condens. Matter 54 (1996) 61–64.
[26] P. Soven, Phys. Rev. 156 (1967) 809–813.
[27] G.M. Stocks, W.M. Temmerman, B.L. Gyorffy, Phys. Rev. Lett. 41 (1978) 339–343.
[28] P.W. Anderson, in: F. Seitz, Turnbull (Eds.), In Solid State Physics, vol. 14, Academic Press, New York, 1963, pp. 99–214.
[29] A.I. Liechtenstein, M.I. Katsnelson, V. Antropov, V.A. Gubanov, J. Magn. Magn Mater. 67 (1987) 65–74.
[30] H. Ebert, S. Mankovsky, Phys. Rev. B Condens. Matter 79 (2009), 045209.
[31] A.M. Ganose, A.J. Jackson, D.O. Scanlon, J. Open Source Softw. 3 (2018) 717.
[32] A. Nozariasbmarz, A. Agarwal, Z.A. Coutant, M.J. Hall, J. Liu, R. Liu, A. Malhotra, P. Norouzzadeh, M.C. Öztürk, V.P. Ramesh, Y. Sargolzaeiaval, F. Suarez, D. Vashaee, Jpn. J. Appl. Phys. 56 (2017), 05DA04.
[33] M.A. McGuire, D.S. Parker, J. Appl. Phys. 118 (2015), 163903.
[34] J. Cedervall, E. Nonnet, D. Hedlund, L. Häggström, T. Ericsson, M. Werwiński, A. Edström, J. Rusz, P. Svedlindh, K. Gunnarsson, M. Sahlberg, Inorg. Chem. 57 (2) (2018) 777–784.
[35] O. Beckman, L. Lundgren 6, Elsevier, 1991, pp. 181–287.
[36] M. Däne, S. Kyung Kim, M.P. Surh, D. Åberg, L.X. Benedict, J. Phys. Condens. Matter 27 (2015), 266002.
[37] P. Haas, F. Tran, P. Blaha, Phys. Rev. B Condens. Matter 79 (2009), 085104.